Evolution of the gas mass fraction in galaxy clusters

Irina Dvorkin, Yoel Rephaeli

HAL Id: insu-03644915
https://insu.hal.science/insu-03644915

Evolution of the gas mass fraction in galaxy clusters

Irina Dvorkin[1,2]★ and Yoel Rephaeli[2,3]

[1]*Institut d'Astrophysique de Paris, UMR 7095, 98 bis boulevard Arago, Paris F-75014, France*
[2]*School of Physics and Astronomy, Tel Aviv University, Tel Aviv 69978, Israel*
[3]*Center for Astrophysics and Space Sciences, University of California, San Diego, La Jolla, CA 92093-0424, USA*

ABSTRACT

The mass fraction of hot gas in clusters is a basic quantity whose level and dependence on the cluster mass and redshift are intimately linked to all cluster X-ray and Sunyayev–Zel'dovich measures. Modelling the evolution of the gas fraction is clearly a necessary ingredient in the description of the hierarchical growth of clusters through mergers of subclumps and mass accretion on the one hand, and the dispersal of gas from the cluster galaxies by tidal interactions, galactic winds and ram-pressure stripping on the other hand. A reasonably complete description of this evolution can only be given by very detailed hydrodynamical simulations, which are, however, resource-intensive and difficult to implement in the mapping of parameter space. A much more practical approach is the use of semi-analytic modelling that can be easily implemented to explore a wide range of parameters. We present first results from a simple model that describes the build-up of the gas mass fraction in clusters by following the overall impact of the above processes during the merger and accretion history of each cluster in the ensemble. Acceptable ranges for model parameters are deduced through comparison with results of X-ray observations. Basic implications of our work for modelling cluster statistical properties, and the use of these properties in joint cosmological data analyses, are discussed.

Key words: galaxies: clusters: general – galaxies: clusters: intracluster medium.

1 INTRODUCTION

Hot intracluster (IC) gas is an important cluster component that determines X-ray emission quantities and the nature and properties of the Sunyaev–Zel'dovich (SZ) effect. Cluster X-ray and SZ surveys provide a broad basis for exploring key statistical properties of the population, such as the mass function, and are valuable cosmological probes of e.g. the equation of state of dark energy, the amplitude of primordial density fluctuations and the neutrino mass (e.g. Vikhlinin et al. 2009; Lueker et al. 2010; Mantz et al. 2010a; Shimon et al. 2012; Planck Collaboration XX 2014). However, both X-ray emission and the SZ signal of a cluster of a given mass are very sensitive to the hot gas mass fraction f_{gas}, which is not known precisely and – in principle – can depend on the mass and redshift of the cluster. While it is expected that f_{gas} should be close to the cosmic value Ω_b/Ω_m by virtue of the large size of clusters, some of the baryons are locked in cluster galaxies, and therefore do not contribute to the respective observable. Therefore, it is of interest to model the fraction of hot, X-ray emitting gas in galaxy clusters, particularly at high redshifts.

Observational effort to determine f_{gas} is motivated also by the basic need to study the evolution of the total baryon fraction in groups and clusters, which has contributions also from galaxies and IC light (e.g. White et al. 1993; Mohr, Mathiesen & Evrard 1999; Ettori 2003; Lin, Mohr & Stanford 2003; Gonzalez, Zaritsky & Zabludoff 2007; McCarthy, Bower & Balogh 2007; Giodini et al. 2009). In several of these works, the reported baryon fraction is smaller than the expected value, particularly in low-mass systems. The observed trend is an increase of the fraction of hot gas with total system mass, approximately following $f_{gas} \propto M^{0.1-0.2}$, and a decrease of the stellar fraction as $f_s \propto M^{-(0.4-0.6)}$ (Lin et al. 2003; Gonzalez et al. 2007; Sun et al. 2009; Dai et al. 2010). A possible interpretation of the mass dependence of f_{gas} is that gas is expelled from low-mass systems due to non-gravitational processes, such as feedback from active galactic nuclei (AGN) (Scannapieco & Oh 2004). In this scenario more massive systems retain a larger fraction of their gas due to their deeper potential wells.

Another important piece of evidence is the observed metallicity of IC gas, with a mean value of $\simeq 1/3$ solar (e.g. Finoguenov, David & Ponman 2000; De Grandi & Molendi 2001; Vikhlinin et al. 2005; Baldi et al. 2012), and with a decreasing radial profile. Since metals are produced only in stars, it follows that a large fraction of IC gas was ejected from galaxies. Indeed, numerical simulations (e.g. Kapferer et al. 2007; Arieli, Rephaeli & Norman 2010) show that ejection of metals from galaxies can account for the observed metallicity. This interpretation is further strengthened by the observed evolution of the galaxies in clusters (the Butcher–Oemler

★ E-mail: irina@wise.tau.ac.il

effect), namely that the fraction of blue galaxies is higher at higher redshifts (Butcher & Oemler 1978); note though that the significance of this effect is uncertain due to difficulties in disentangling the influence of the chosen galaxy sample and secular evolution (Raichoor & Andreon 2012). Moreover, spirals found in clusters tend to be redder (Hughes & Cortese 2009), H I deficient as compared to similar galaxies in the field (Solanes et al. 2001), and typically have truncated gaseous discs (Koopmann, Haynes & Catinella 2006). These observations suggest that galaxies lost most or all of their gas since they first fell into the cluster, either due to encounters with other galaxies, or as a result of ram-pressure stripping, as discussed below. This led to the quenching of star formation and the subsequent change of colour and morphology.

The baryonic fraction in clusters, particularly the fraction of hot gas, was extensively studied using cosmological hydrodynamical simulations (e.g. Borgani et al. 2006; Ettori et al. 2006; Stanek et al. 2010; Young et al. 2011; Planelles et al. 2013). While the observed mass dependence of f_{gas} is generally well reproduced by these simulations, the stellar mass fraction is typically larger than observed, which may be due to the fact that the (correct) gas mass fraction is attained by an overestimated star formation rate (SFR). In general, numerical simulations are computationally expensive, which complicates the modelling of the interplay between galactic and large-scale phenomena.

An alternative semi-analytic model, proposed by Bode, Ostriker & Vikhlinin (2009, see also Ostriker, Bode & Babul 2005), is based on the assumption that f_{gas} in all haloes was initially equal to the cosmic baryon fraction, and that it decreased due to the processes of star formation and ejection of gas out of the halo by SN-and-AGN-driven winds. This model is calibrated to X-ray observations of nearby clusters, and so successfully reproduces the local cluster population.

In this paper, we take a different approach: motivated by the observed metallicity and galaxy (colour) evolution, we assume that a large fraction of the IC gas was ejected from galaxies. In this picture f_{gas} increases with mass because larger systems typically form later through mergers of smaller systems, and therefore their galaxies had more time to eject their gas. As we show in this paper, our model directly links galactic processes (which can be described by small-scale numerical simulations) with various cluster-scale observables.

Several processes may be responsible for mass ejection from cluster galaxies. When a galaxy traverses the higher density inner region of a cluster, ram pressure effectively removes an appreciable fraction of its interstellar (IS) gas (Gunn & Gott 1972). The details of this process depend on the IC gas density profile, galactic gas density profile and the trajectory of the galaxy (Abadi, Moore & Bower 1999; Vollmer et al. 2001; Hester 2006; Tecce et al. 2010), all of which are difficult to model, but it is clear that ram pressure can remove large quantities of gas from the galaxy on relatively short time-scales (e.g. Quilis, Moore & Bower 2000). Observational evidence for this process comes from the tails behind several cluster galaxies seen in H I, H α and X-rays, interpreted as removal of galactic interstellar medium (ISM; e.g. Sun, Donahue & Voit 2007; Ebeling, Stephenson & Edge 2014). In addition, tidal interactions between field galaxies are known to affect the distribution of gas and stars within the galaxies, and may be as important in cluster galaxies, especially in dense cluster cores (Merritt 1983; Moore et al. 1999; Gnedin 2003). Tidal interactions truncate the dark matter (DM) density profile of subhaloes orbiting inside a massive cluster, which leads to more concentrated profiles of subhaloes relative to field haloes (Bullock et al. 2001; Limousin et al. 2009). The

transformation of spirals into S0 galaxies in clusters and the existence of 'passive spirals' (which are morphologically identical to normal spirals but lack star formation activity) may be related to these environmental effects (e.g. Bekki, Couch & Shioya 2002; Just et al. 2010).

Other major processes that affect galaxy evolution in clusters are galactic winds and AGN feedback. SN-driven winds are particularly important at high redshifts, when the SFR is high (e.g. Pettini et al. 2001). A sufficiently fast wind deposits metal-enriched material into IC space. However, as the SFR drops at low redshifts, metal enrichment effects of galactic winds become subdominant to ram pressure and tidal interactions.

Outflows launched from the vicinity of supermassive black holes found in the central galaxies of clusters may provide the IC gas with enough energy to escape the cluster potential well and thus lower the IC gas mass fraction (see e.g. Fabian 2012, for a comprehensive discussion of the role of AGN in clusters). X-ray cavities in the central regions of many clusters, often found in pairs, provide strong evidence of these outflows. Their ubiquity is, however, a matter of debate. The detection fraction of X-ray cavities is between 20 and 30 per cent in X-ray-selected samples (Bîrzan et al. 2004; Dunn, Fabian & Taylor 2005; Hlavacek-Larrondo et al. 2012). On the other hand, a recent study by Hlavacek-Larrondo et al. (2014) found only six clusters with X-ray cavities in a sample of 83 massive clusters selected by their SZ signature. While the detection of X-ray cavities is observationally challenging due to their small contrast with the surrounding medium, their contribution to the overall properties of the cluster population (rather than individual clusters with extremely strong outflows) remains an open question. Moreover, while the energy deposited into the IC gas is probably sufficient to prevent overcooling (McNamara & Nulsen 2007), it is not clear that large amounts of gas can also escape the potential well of the clusters.

In view of these findings we focus here on environmental processes which are widespread in galaxy clusters and are closely related to their mass accretion histories.

In this paper, we build a phenomenological model of gas ejection in the context of the hierarchical assembly of clusters and explore the range of possible models and their consequences for X-ray and SZ cluster surveys. We adopt the following cosmological parameters: $H_0 = 67.11 \, \mathrm{km \, s^{-1} Mpc^{-1}}$, $\Omega_m = 0.3175$, $\Omega_\Lambda = 0.6825$, $\sigma_8 = 0.8344$ and $n_s = 0.9624$ (Planck Collaboration XVI 2014). Unless otherwise stated, all masses M and radii R represent the virial quantities, defined by $M = 4\pi/3 \, \Delta_V \rho_c(z) R^3$, where ρ_c is the critical density of the Universe at redshift z and Δ_V is the overdensity defined by the spherical collapse model (Gunn & Gott 1972) calculated for the given set of cosmological parameters.

In Section 2, we briefly describe our model of cluster evolution, which is based on an extended merger-tree code that follows the evolution of haloes that consist of DM and baryons. Gas ejection from galaxies and the build-up of f_{gas} is discussed in Section 3. Our results are presented in Section 4 and discussed in Section 5.

2 CLUSTER MERGER-TREE EVOLUTION

The efficiency of IS gas removal by tidal interactions and ram pressure depends on the depth of the cluster gravitational potential. This occurs continuously through a series of interaction and merger events during the dynamical evolution of a galaxy in a growing cluster. We follow the evolutionary history of IC gas by considering the overall impact of the above galactic processes in a statistical description based on a merger-tree code.

In the Λ cold dark matter framework structure forms hierarchically, starting with relatively low mass haloes that grow successively through mergers and accretion. The merger history of a given cluster can be described by a *merger tree*, which essentially is a list of the masses of the merging haloes and the redshifts at which these mergers occurred. The mass assembly history of a cluster affects its density profile (Wechsler et al. 2002; Dalal, Lithwick & Kuhlen 2010) and causes an intrinsic scatter in all the mass-observable relations. In previous works (Dvorkin & Rephaeli 2011; Dvorkin, Rephaeli & Shimon 2012), we studied how the hierarchical formation of galaxy clusters affects their X-ray and SZ properties; here we extend our merger-tree approach to include an approximate description of some basic galaxy-scale processes.

In order to describe the evolution of galaxy clusters we build merger trees of DM haloes using the GALFORM algorithm (Parkinson, Cole & Helly 2008) which is based on the excursion set formalism (Lacey & Cole 1993). For a cluster with a given mass and at a given observation redshift each merger tree represents a possible formation history, and a sufficiently large number of merger trees can provide a statistical description of the population. The advantage of using this kind of semi-analytic modelling is our ability to produce a large number of clusters (equivalent to simulating a very large volume of the Universe) by employing an efficient algorithm that can be readily applied to explore the parameter space of the model.

Instead of using a constant redshift step for the output of the merger tree, we save the information on all the progenitors with masses $M > M_{res}$, where M_{res} is the mass resolution limit. The merger trees of Parkinson et al. (2008) are calibrated to match the Sheth–Tormen mass function (Sheth & Tormen 1999), which we use throughout this paper for consistency. The original DM-only merger-tree code was extended to include also IC gas, whose density and temperature profiles are determined from basic considerations (essentially, energy conservation and hydrostatic equilibrium). Further details on the merger-tree algorithm and its implementation for clusters of galaxies can be found in Parkinson et al. (2008) and Dvorkin & Rephaeli (2011).

We follow the evolution of all haloes in a tree (i.e. all the progenitors of the given cluster) with (total) masses $M > M_{res} = 10^{11} \, \mathrm{M_\odot} \, h^{-1}$ that existed below redshift $z = 2$. The number of galaxies in a halo scales linearly with its mass M, therefore we calculate the initial number of galaxies in each halo as

$$N_{gal,i}(M) = N_{gal,0} \left(\frac{M}{10^{11} \, \mathrm{M_\odot} \, h^{-1}} \right), \qquad (1)$$

where $N_{gal,0}$ is a model parameter. At high enough redshift large structures are rare; therefore, their member galaxies are expected to resemble low-redshift galaxies in the field, i.e. they should be relatively massive blue discs. We assign an initial mass for these galaxies $M_{gal,i} = 10^{11} \, \mathrm{M_\odot} \, h^{-1}$, a value that decreases by the various mass-loss processes.

An alternative method of describing the galaxy population would be to explicitly account for subhaloes and follow them as distinct systems even after they merge with the main halo. This kind of approach (i.e. Yoo et al. 2007) necessitates modelling the trajectory of each galaxy inside the main halo, taking into account dynamical friction, encounters with other subhaloes, and the impact of subsequent mergers of the main halo with other systems. While this kind of approach provides a more accurate description of cluster growth, it might be difficult to pinpoint the key physical processes that influence the evolution of IC gas. Therefore, we chose to assign all the galaxies the same (fiducial) initial mass, which is reduced at later stages of evolution as described below. We note that our model

effectively averages over all possible galaxy masses and trajectories, as well as the merger impact parameters.

The gas mass fraction in the diffuse matter that was not contained in collapsed structures (this gas could originate from early galactic winds) is f_{diff} at the initial time, so that $M_{gas,i} = f_{diff} \cdot (M - M_{gal,i} N_{gal})$, whereas galaxies are assumed to have the cosmic baryon fraction $f_c = \Omega_b / \Omega_m$. Clearly, baryon ejection processes from galaxies affect the stellar component, the disc, and the warm gas in the galactic halo.

3 MODELING IC ENVIRONMENTAL PROCESSES

When galaxies fall on to larger structures, they experience tidal interactions with the host halo and other subhaloes. The strength of these interactions depends on the host halo mass, or on the local density of galaxies, which is ultimately also determined by the host mass. Tidal interactions affect the DM, as well as IS gas, so that cluster galaxies are expected to have truncated DM profiles (Limousin et al. 2009). This truncation enhances the effect of ram-pressure stripping by making the galaxy potential wells effectively shallower.

Numerical simulations show that the time-scale of gas removal from galaxies through ram pressure is relatively short (Quilis et al. 2000), and that the fraction of gas-depleted galaxies is a strong function of host halo mass (Hester 2006; Tecce et al. 2010). Thus, although the ram pressure experienced by a galaxy moving in a cluster varies between a maximal value attained at the cluster centre and a minimal value in the outskirts (Brüggen & De Lucia 2008), most loosely bound gas is likely to be ejected upon first passage through the centre. Further stripping occurs when the galaxy is in a deeper potential well, i.e. after a merger with a larger halo. This episodic mass-loss and the connection between ram-pressure stripping and the merging history of the cluster is demonstrated by the numerical simulations of Kapferer et al. (2007). On the other hand, the model by Hester (2006) shows that for a galaxy of a given mass there exists a limiting cluster mass for which ram pressure is strong enough to remove almost all of the gas even in the innermost regions of the galaxy, while for smaller cluster masses almost none of the gas is removed.

Motivated by these findings, we assume that the efficiency of gas removal is a power law in cluster mass. If this dependence is steep, all available gas will be removed from the galaxies once the cluster reaches a certain mass, resulting in gas mass fraction which is roughly a step-function in cluster mass. On the other hand, if the efficiency is only weakly dependent on cluster mass, gas will be removed from galaxies in a more gradual manner. We stress that this is a phenomenological model intended to link the observable properties of galaxy clusters to galactic processes. In other words, our model parameters, in particular those related to the efficiency of gas removal, provide the basis for an effective description of more complex galactic processes. We briefly discuss how our model can be used to study these processes in Section 5.

Our calculation proceeds as follows. After each merger event a fraction

$$f_m = f_{m,0} \left(\frac{M}{10^{14} \, \mathrm{M_\odot} \, h^{-1}} \right)^{\alpha} \qquad (2)$$

of the total galactic mass is removed, of which f_c is in baryons:

$$\Delta M_{gas} = f_m f_c N_{gal} M_{gal} . \qquad (3)$$

This gas is no longer bound to the galaxy and is assumed to immediately mix with the IC gas. In equation (3), M is the halo mass,

N_{gal} is given in equation (1) and M_{gal} is the mass of a typical galaxy residing in this halo. This mass is reduced after each merger event to account for the mass-loss as follows:

$$M_{\mathrm{gal}} \rightarrow M_{\mathrm{gal}} \cdot (1 - f_{\mathrm{m}}). \qquad (4)$$

The parameter α describes the steepness of the dependence of gas removal on cluster mass; for large values of α there will be a very pronounced transition from insignificant environmental effects to very rapid mass ejection from the galaxy, whereas for small values of α the ejection process is more gradual.

We approximate the virialization phase of gas removed from galaxies by assuming that it is immediately heated to the virial temperature of the host halo. Thus, the hot gas content of a halo immediately after a merger event is

$$M_{\mathrm{gas}}(M) = M_{\mathrm{gas}}(M_1) + M_{\mathrm{gas}}(M_2) + \Delta M_{\mathrm{gas}} + \Delta M_{\mathrm{gas,diff}}, \qquad (5)$$

where M_1, M_2 are the masses of the two merging haloes (typically the host halo and a smaller halo), ΔM_{gas} is calculated as in equation (3) and $\Delta M_{\mathrm{gas, diff}}$ is the gas contained in diffuse matter that falls on to the halo. This last term is given by $\Delta M_{\mathrm{gas, diff}} = f_{\mathrm{diff}} M_{\mathrm{diff}}$, where M_{diff} is the mass contained in haloes below the resolution limit M_{res} of the merger tree (see Section 2).
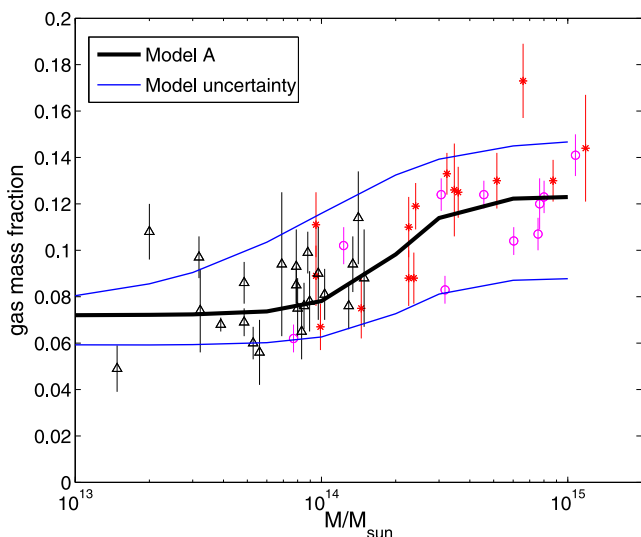
These equations are employed following each merger event, so that the gas content of the cluster increases as the cluster evolves and the mean mass of cluster galaxies is decreased.

4 RESULTS

4.1 IC gas fraction and metallicity

We ran 1000 tree realizations for each halo mass with mass resolution of $M_{\mathrm{res}} = 10^{11}\,\mathrm{M_{\odot}}\,h^{-1}$ and up to $z = 2$. We considered all merger events between haloes above this resolution mass. Mergers with smaller haloes were considered as part of the smooth accretion process, as described above.

Fig. 1 shows the hot gas mass fraction in clusters in the mass range $10^{13}\,\mathrm{M_{\odot}}\,h^{-1}$–$10^{15}\,\mathrm{M_{\odot}}\,h^{-1}$ as predicted by our model, and

Table 1. Parameter values used for the fiducial model *A* (solid black curve in Figs. 1–3); representative models *B* and *C* (dashed red curve and dot–dashed magenta curve, respectively), and the lower and upper ranges of the models, A_{min} and A_{max}, depicted as thin blue lines in Fig. 1.

	A	*B*	*C*	A_{min}	A_{max}
$N_{\mathrm{gal,0}}$	0.5	0.3	0.5	0.3	0.7
f_{diff}	0.11	0.12	0.12	0.0725	0.14
$f_{\mathrm{m,0}}$	0.01	0.01	0.01	0.01	0.045
α	1.84	1.0	0.7	1.55	0.39

Table 2. Parameter values for the fit in equation (6) for the different models discussed in the text. Note that the physical parameters that define the models are given in Table 1. The transition to efficient mass stripping occurs at around $M = 10^a\,\mathrm{M_{\odot}}$ for each model.

	A	*B*	*C*	A_{min}	A_{max}
a	14.29	13.87	14.45	14.32	13.95
b	0.135	0.189	0.251	0.148	0.295
c	0.051	0.028	0.053	0.029	0.071
d	0.072	0.099	0.081	0.059	0.078

compared with data from several X-ray studies. Parameters of the fiducial model, shown in black, are given in Table 1. We compare our model with X-ray observations of groups and clusters (points with error-bars) and find good agreement. These results suggest that the mass dependence of f_{gas} can be largely explained by environmental processes. To obtain an estimate for the range of parameter values that are consistent with the data, we show by the thin blue lines in Fig. 1 the approximate region that brackets the range of values of the three data sets. These upper and lower lines correspond to models A_{max} and A_{min}, respectively, whose parameters are given in Table 1. Note though that the comparison with observations has only a limited value due to substantial modelling uncertainty, mainly in the cluster mass determination from X-ray observables.
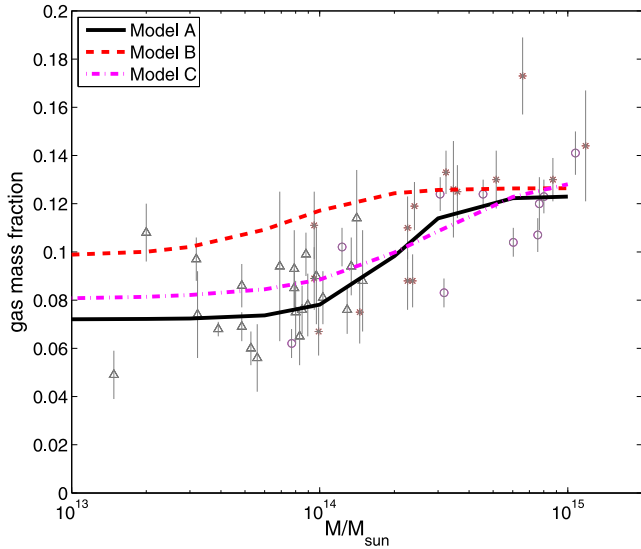
An analytical fit to the fiducial model is

$$f_{\mathrm{gas}} = c \left(1 + \mathrm{e}^{-\left[\log_{10}(M/\mathrm{M_{\odot}}) - a \right]/b} \right)^{-1} + d \,. \qquad (6)$$

The fit parameters for the models shown on Fig. 1 are given in Table 2. The fit demonstrates the transition to efficient mass stripping, which occurs around $M = 10^a\,\mathrm{M_{\odot}}$.

No explicit redshift dependence is deduced from our results, in line with the usual assumptions (e.g. Allen et al. 2008). The reason for this is that in our model the efficiency of gas removal from cluster galaxies depends on the mass of the host halo, but not explicitly on the redshift at which galaxy infall occurs. Note though that the dependence on mass clearly introduces implicit redshift dependence through the strong mass dependence of the probability distribution function of cluster formation times (e.g. Sadeh & Rephaeli 2008).

Fig. 2 shows the results of our model for three representative sets of parameters: Model A (the fiducial model shown on Fig. 1; solid black line), Model B (dashed red line) and Model C (dot–dashed magenta line). The corresponding parameters are given in Table 1. In all three models the gas mass fraction increases with mass by $\sim$20–50 per cent from groups to rich clusters, respectively. This trend is largely determined by the following model parameters: $N_{\mathrm{gal,\,0}}$, which

Figure 1. Gas mass fraction versus cluster mass for the fiducial model (thick black line) with model uncertainty range bracketed by the thin blue lines. Parameter values are specified in Table 1. X-ray measurements inside M_{500} from Gonzalez et al. (2013, red stars), Vikhlinin et al. (2006, magenta circles) and Sun et al. (2009, black triangles).

Figure 2. Gas mass fraction versus cluster mass for three representative models (see Table 1 for the parameters used in each case). Points with error bars show the X-ray measurements, specified in the caption of Fig. 1.

Figure 3. Metal abundance (in units of the solar value) for models A, B and C for which the corresponding f_{gas} is shown in Fig. 2.

is related to the amount of gas initially locked inside galaxies, and f_{diff}, which is the gas fraction in diffuse matter. The latter parameter is expected to be high, but lower than the universal value f_c since baryons are more clustered than DM. The parameters $f_{m,0}$ and α quantify the environmental processes that galaxies undergo as the cluster is assembled and affect the transition from the low f_{gas} level in groups to a high level in rich clusters. In particular, the steepness of this transition is determined by the value of α (see equation 2).

While a more complete and quantitative description of gas ejection processes requires a high spatial resolution hydrodynamical simulation that can follow individual galaxy trajectories, our simple treatment seems to provide an adequate basis for comparison with the data. The good agreement of the predicted mass dependence of f_{gas} with the observations clearly indicates that *on average* cluster environmental processes may be described by a few universal model parameters. Interestingly, the observed f_{gas} exhibits large scatter, which may be linked to the scatter in these unresolved parameters. Quantifying the connection between the varying galactic trajectories, composition, IC gas density profile, values of the merger impact parameter, and the scatter in our effective model parameters, is an important future goal (which is clearly beyond the scope of our simplified treatment).

IC gas metallicity provides additional insight on the evolution of the gas mass fraction. Gas that was removed from galaxies obviously has higher metal abundance than the intercluster gas. However, the metallicity of the latter which we denote by Z_i could be higher than that of primordial gas, since it could have already been enriched by galactic outflows (Werner et al. 2013). On the other hand, the metallicity of galactic gas, Z_{gal} depends on the stellar mass and probably also on the environment of the galaxy (Peng & Maiolino 2014). Since these parameters depend on processes that occurred before $z = 2$, long before the cluster had assembled, we do not attempt to model them here, instead we adopt effective constant values for both Z_i and Z_{gal}.

Fig. 3 shows the metallicity of the IC gas for various cluster masses with $Z_i = 0.1$ and $Z_{gal} = 0.8$. It can be seen that although all three models produce similar $f_{gas}(M)$ they can be further distinguished by their very different mass-metallicity relations (which,
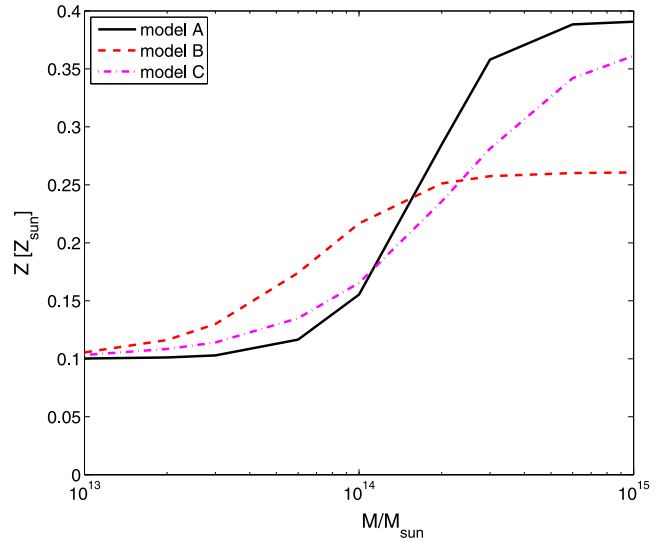
however, depend on the assumed ratio of Z_i/Z_{gal}. The differences between the selected models are mostly evident for the most massive clusters, but also for $M \lesssim 10^{14}\,\mathrm{M_\odot}$ which roughly corresponds to the halo mass for which environmental effects become important. Interestingly, there seems to be some observational evidence (Rasmussen & Ponman 2009; Sasaki, Matsushita & Sato 2014) for an increase of the mean metal abundance with IC gas temperature, and hence with system mass (although other studies, e.g. Zhang et al. 2011 and Baldi et al. 2012, favour an inverse trend). We caution, however, that current X-ray studies measure the metal abundance in the innermost region of the cluster, typically inside R_{500} or less, due to observational difficulties, and the evolution of the central metal abundance might differ appreciably from the evolution of the total metallic mass in the cluster. Further investigation of the chemical composition of IC gas in groups and clusters will help constrain our model and provide more information on the processes of gas enrichment.

4.2 X-ray luminosity

Modelling $f_{gas}(M)$ is particularly important in view of the ongoing and upcoming X-ray and SZ cluster surveys, whose main objectives are the study of cluster properties and the use of clusters as precise cosmological probes. These surveys, when jointly analysed together with complementary cosmological probes (such as CMB anisotropies and baryonic acoustic oscillations) can shed light on the physics of galaxy clusters and the nature of mass-observable relations. The latter are shaped by cosmological structure formation, as well as small-scale physics. Therefore, the magnitude of f_{gas} and its $M \& z$ dependence may effectively serve as a means of studying the main physical processes affecting galaxies in dense environments, provided the cosmological parameters are constrained fairly well by complementary probes. In particular, the f_{gas} models proposed here can be used to link X-ray observables to galactic processes in clusters.

First, we calculate the scaling relation between the bolometric X-ray luminosity and the emission weighted temperature inside R_{500}. In order to calculate the density and temperature profile we assume a polytropic model (e.g. Ascasibar et al. 2003), so that the pressure and density are related by $P = P_0(\rho/\rho_0)^\Gamma$ with $\Gamma = 1.2$. Then the
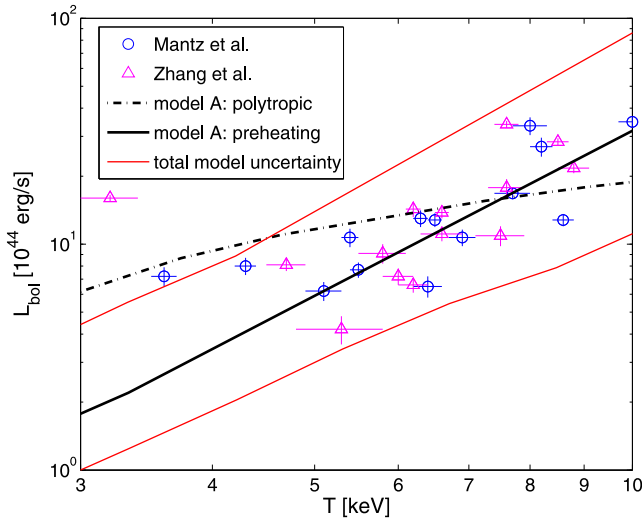
Figure 4. Bolometric luminosity–temperature relation computed using the polytropic f_{gas} model (dot–dashed black line), preheating model with a uniform entropy floor of 150 keV cm^2 (solid black line) and model uncertainty region (thin red lines) compared with X-ray measurements from Zhang et al. (2008) and Mantz et al. (2010b).

Figure 5. X-ray luminosity function computed using the fiducial f_{gas} model (thick black line) and model uncertainty region (thin red lines) for clusters in the range $z = 0$–0.5. The luminosity is calculated for the 0.1–2.4 keV spectral band.

solution of the equation of hydrostatic equilibrium for a polytropic gas inside a potential well of a DM halo with an NFW profile is (Ostriker et al. 2005)

$$\rho(x) = \rho_0 \left[1 - \frac{B}{1+n} \left(1 - \frac{\ln(1+x)}{x} \right) \right]^n, \qquad (7)$$

where $n = (\Gamma - 1)^{-1}$, $B = 4\pi G \rho_s r_s^2 \mu m_p / k_B T_0$, μm_p is the mean molecular weight, $r_s = R/c$ is the scale radius of the cluster and c is the concentration parameter of the DM halo. The temperature profile is given by

$$T(x) = T_0 \left[1 - \frac{B}{1+n} \left(1 - \frac{\ln(1+x)}{x} \right) \right]. \qquad (8)$$

We take the halo concentration parameters from our merger-tree model, which describes the DM density profile as a function of the formation history of the cluster (Dvorkin & Rephaeli 2011; Dvorkin et al. 2012).

Fig. 4 shows the bolometric luminosity L_X versus emission weighted temperature for model clusters at $z = 0$ compared with low-redshift observations with the polytropic model shown by the dot–dashed black line. While the model prediction reasonably agrees with the data, the slope of the luminosity–temperature relation is too shallow and follows the self-similar prediction $L \propto T^2$, instead of the observed $L \propto T^3$. This discrepancy clearly stems from our simplistic description of IC gas equation of state. Quite possibly, this discrepancy indicates the need for additional energy input from supernovae, galactic winds or AGN which are related to the cluster galactic evolutionary processes. These lead also to the overall effect of gas preheating, as has been proposed in various preheating models (e.g. Bialek, Evrard & Mohr 2001; Babul et al. 2002; Voit et al. 2003). This calculation is beyond the scope of this paper and we leave it to future work. However, in order to demonstrate the effect of this preheating we include a simple model, based on the work of Younger & Bryan (2007) and described in the appendix, where we assume a constant entropy floor for all clusters. This assumption amounts to uniformly raising the entropy level of all intergalactic gas well before the formation of groups and clusters. Since possible sources of preheating are related to star formation, which peaks at
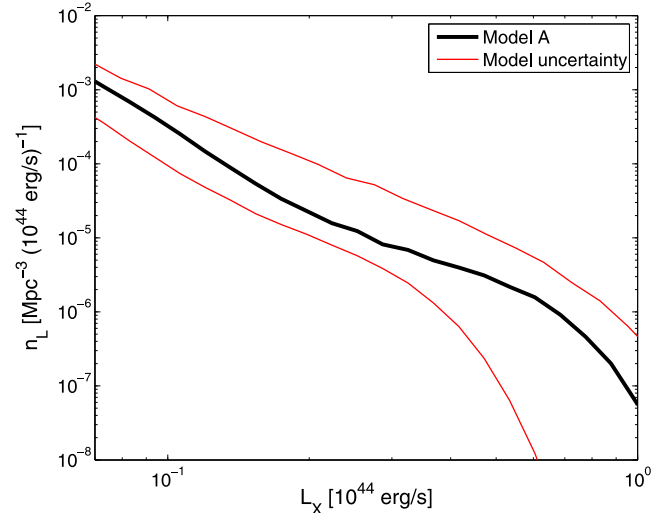
$z \sim 2$, this assumption is fairly reasonable. Nevertheless, this description is not entirely self-consistent if energy injection continues also at lower redshifts, as we do not consider the effects of gas ejection from groups due to increased entropy, which could affect the evolution of the gas mass fraction. Indeed, there are observational hints for the connection between the gas mass fraction and the entropy profile (Pratt et al. 2010). (In Section 5, we briefly outline our plan for a more fully consistent treatment of preheating in our merger-tree approach.)

The solid black curve in Fig. 4 shows the results of the preheating model, where we assumed an entropy floor of $K_0 = 150$ keV cm^2. This model clearly provides a much better fit to observations. Note, however, that there is a significant dispersion in the observed entropy floor (Pratt et al. 2010; McDonald et al. 2014). In the absence of a complete model that follows the development of this entropy excess in each individual cluster, we explore a plausible range of values for K_0. The thin red curves in Fig. 4 mark the estimated range resulting from the uncertainty in the gas mass fraction model (blue curves in Fig. 1) and in the entropy floor: $K_0 = 100$–200 keV cm^2. This combined uncertainty brackets the observations, as expected. The observed scatter in the X-ray scaling relations might be due to different dynamical state of some of the clusters (i.e. they could be out of equilibrium due to a recent merger event), as well as variations in f_{gas}.

Having demonstrated the viability of the preheating assumption for our model we use the simple polytropic case in the remainder of this paper in order to isolate the effects of our IC gas model.

Additional information is provided by the cluster luminosity function. Recently, Böhringer, Chon & Collins (2014) used the REFLEX II cluster survey to construct the X-ray luminosity function and to derive constraints on Ω_m and σ_8. Future surveys will be able to extend this analysis to higher redshifts, probing the mass function and thermodynamical properties of these systems.

Fig. 5 shows the expected luminosity function for redshifts up to $z = 0.5$ in the measured 0.1–2.4 keV spectral band, which corresponds to the energy range of *ROSAT* measurements. We used the Sheth–Tormen mass function for consistency with the merger-tree algorithm we employ. In future, we plan to extend this work

by calibrating the merger-tree building code to more general mass functions, so as to carry out a more detailed comparison with results of hydrodynamical simulations.

4.3 SZ power spectrum

Recent findings by the Planck Collaboration XX (2014) indicate that there is 'tension' between the observed SZ power spectrum and cluster number counts and theoretical predictions based on primary cosmic microwave background (CMB) observations. One of the possible culprits is the gas mass fraction, which links the DM halo abundance, predicted by theory, to the observed SZ signal, which results from interaction of CMB photons and hot IC electrons. It is quite interesting, therefore, to check whether our range of f_{gas} models can alleviate the tension reported by *Planck*.

We compute the SZ power spectrum using the halo approximation (Komatsu & Seljak 2002):

$$C_\ell = s(\chi)^2 \int_0^{z_{max}} \frac{dV(z)}{dz} dz \int_{M_{min}}^{M_{max}} dM \frac{dn}{dM} |y_\ell(M, z)|^2, \qquad (9)$$

where $s(\chi)$ is the spectral dependence of the SZ signal given by

$$s(\chi) = \chi \frac{e^\chi + 1}{e^\chi - 1} - 4, \qquad (10)$$

$\chi = h\nu/k_B T_0$ is the dimensionless frequency, $V(z)$ is the comoving volume per steradian, and dn/dM is the mass function. The 2D Fourier transform of the projected Comptonization parameter is

$$y_\ell = \frac{4\pi r_s}{\ell_s^2} \int_0^c dx \, x^2 \frac{\sin(\ell x/\ell_s)}{\ell x/\ell_s} \zeta(x), \qquad (11)$$

where $\ell_s = d_A(z)/r_s$, $d_A(z)$ is the angular diameter distance to the cluster and $\zeta(x)$ is the gas (normalized) pressure

$$\zeta(x) = \frac{k_B \sigma_T}{m_e c^2} n_e(x) T_e(x). \qquad (12)$$

Typical parameters are $z_{max} = 2$, $M_{min} = 10^{13} \, h^{-1} \, M_\odot$ and $M_{max} = 10^{16} \, h^{-1} \, M_\odot$. The concentration parameter is calculated as above, using our merger-tree model of cluster evolution. The temperature and density profiles are given by equations (7) and (8).

The resulting thermal SZ power spectrum is shown in Fig. 6. Given the cosmological parameters deduced from primary CMB observations by *Planck* (adopted in this work) our fiducial model
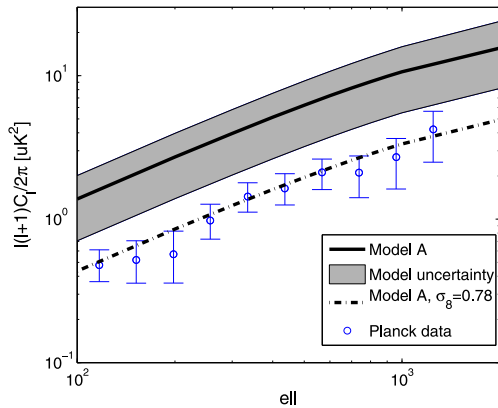
Figure 6. SZ power spectrum for the fiducial model (black line) and the model uncertainty region (grey stripe) that corresponds to the blue lines on Fig. 1. Also shown are measurements from *Planck* (blue circles), and the fiducial model with $\sigma_8 = 0.78$, which corresponds to the lower 2σ limit of the constraint from *Planck* (dot–dashed black line).

is in tension with *Planck* measurements of the SZ power spectrum. This result reflects the $\sim 2\sigma$ discrepancy between the values of σ_8 and Ω_m deduced from primary CMB versus cluster number counts (Planck Collaboration XX 2014). We demonstrate the important implication of this discrepancy by the dashed black line in Fig. 6, calculated with our fiducial f_{gas} model and $\sigma_8 = 0.78$, which corresponds to the 2σ lower limit of the *Planck* primary CMB value. It is apparent, then, that the uncertainty in the value of σ_8 can largely explain the discrepancy with the deduced SZ power spectrum, even if other additional uncertainties in cluster parameters (such as the mass function and the gas equation of state) are ignored.

5 DISCUSSION

We developed a simple and efficient model that accurately describes the mass dependence of the hot gas mass fraction in clusters. Our model links two important physical phenomena: the morphological transformation (and mass-loss) of cluster galaxies under the influence of the dense cluster environment, and the evolution of the hot gas. Our results show that the possible relation between these processes can be understood in terms of a few parameters with intuitive physical interpretation: the amount of galaxies, the gas fraction of diffuse matter and the efficiency of gas removal from galaxies which we modelled as a power law in halo mass. At present, none of these parameters is known with high precision; detailed hydrodynamical simulations are needed in order to determine the properties of high-redshift galaxies and to better understand the IC processes that affect the evolution of their IS gas.

However, our model offers an alternative way to understand IC gas evolution through comparison with the observed f_{gas} and metallicity. While it is computationally challenging to develop and run hydrodynamical simulations of cosmological structure formation that also resolve structure and (relatively) small-scale galactic processes, such as ram-pressure stripping, our approach provides a convenient framework for studying the important gas ejection processes. A general model can be derived by fitting $f_{gas}(M)$ measurements, as demonstrated above. This model predicts specific dependence of the efficiency of gas removal from galaxies, which can be tested against small-scale numerical simulations of ram-pressure and tidal stripping, processes whose quantitative assessment does not require the full framework of a cosmological simulation. Such simulations can be run with different galactic masses and ambient IC gas densities to study how these parameters contribute to the scatter in $f_{m, 0}$ and α that control gas removal efficiency in our model. Additional constraints can be provided by measurements of IC gas metallicity, as demonstrated in the previous section.

An important and timely application of our simple numerical approach is the prediction of the SZ power spectrum. We reproduce the $\sim 2\sigma$ discrepancy between the models based on cosmological parameters deduced from primary CMB observations, and the observationally deduced (by *Planck*) thermal SZ power spectrum. While the range of model parameters adopted here do not seem to resolve this discrepancy, the insight gained from our treatment can be useful in future studies of the SZ effect, which will allow better assessment of the uncertainties resulting from IC gas physics.

It is a well-known fact that preheating models which assume a uniform entropy floor provide a better description of the observed luminosity–temperature relation than the simple polytropic model. Nevertheless, the nature of the preheating sources is still debated. Interestingly, the degree of preheating and its impact on the equation of state might be related to the IC gas enrichment processes we discuss here. In particular, if preheating occurs due to galactic winds,

which also carry metals, we would expect a correlation between the entropy floor and metal abundance, whereas if the main preheating source is feedback from AGN no such correlation is expected. In addition, non-uniform preheating should influence the gas mass fraction by expelling the gas out of less massive systems. This possibility is explored in Ostriker et al. (2005) and Bode et al. (2009). In future work, we plan to extend our model to account for energy, as well as mass ejection from cluster galaxies, and to use the framework developed in this paper to distinguish between different preheating scenarios.

We plan to further extend this work by implementing different mass functions and thereby providing much more accurate calculations of the cluster statistical measures. Another route of investigation is the introduction of cluster-to-cluster scatter in our model parameters. The ultimate goal is constraining our model parameters and their scatter using the observables discussed above – $f_{gas}(M)$, metallicity, X-ray scaling relations and luminosity function and SZ power spectrum – and providing a handle on the details of the environmental processes that mostly affect cluster galaxies. These results can be used as an input, or compared against, small-scale simulations of galaxies in an ambient gas environment, where the modelling of galactic structure and dynamics inside the cluster can be controlled.

ACKNOWLEDGEMENTS

REFERENCES

Abadi M. G., Moore B., Bower R. G., 1999, MNRAS, 308, 947
Allen S. W., Rapetti D. A., Schmidt R. W., Ebeling H., Morris R. G., Fabian A. C., 2008, MNRAS, 383, 879
Arieli Y., Rephaeli Y., Norman M. L., 2010, ApJ, 716, 918
Ascasibar Y., Yepes G., Müller V., Gottlöber S., 2003, MNRAS, 346, 731
Babul A., Balogh M. L., Lewis G. F., Poole G. B., 2002, MNRAS, 330, 329
Baldi A., Ettori S., Molendi S., Balestra I., Gastaldello F., Tozzi P., 2012, A&A, 537, A142
Bekki K., Couch W. J., Shioya Y., 2002, ApJ, 577, 651
Bialek J. J., Evrard A. E., Mohr J. J., 2001, ApJ, 555, 597
Bîrzan L., Rafferty D. A., McNamara B. R., Wise M. W., Nulsen P. E. J., 2004, ApJ, 607, 800
Bode P., Ostriker J. P., Vikhlinin A., 2009, ApJ, 700, 989
Böhringer H., Chon G., Collins C. A., 2014, A&A, 570, A31
Borgani S. et al., 2006, MNRAS, 367, 1641
Brüggen M., De Lucia G., 2008, MNRAS, 383, 1336
Bullock J. S., Kolatt T. S., Sigad Y., Somerville R. S., Kravtsov A. V., Klypin A. A., Primack J. R., Dekel A., 2001, MNRAS, 321, 559
Butcher H., Oemler A., Jr, 1978, ApJ, 219, 18
Dai X., Bregman J. N., Kochanek C. S., Rasia E., 2010, ApJ, 719, 119
Dalal N., Lithwick Y., Kuhlen M., 2010, preprint (arXiv:1010.2539)
De Grandi S., Molendi S., 2001, ApJ, 551, 153
Dunn R. J. H., Fabian A. C., Taylor G. B., 2005, MNRAS, 364, 1343
Dvorkin I., Rephaeli Y., 2011, MNRAS, 412, 665
Dvorkin I., Rephaeli Y., Shimon M., 2012, MNRAS, 421, 2648
Ebeling H., Stephenson L. N., Edge A. C., 2014, ApJ, 781, L40
Ettori S., 2003, MNRAS, 344, L13
Ettori S., Dolag K., Borgani S., Murante G., 2006, MNRAS, 365, 1021

Fabian A. C., 2012, ARA&A, 50, 455
Finoguenov A., David L. P., Ponman T. J., 2000, ApJ, 544, 188
Giodini S. et al., 2009, ApJ, 703, 982
Gnedin O. Y., 2003, ApJ, 582, 141
Gonzalez A. H., Zaritsky D., Zabludoff A. I., 2007, ApJ, 666, 147
Gonzalez A. H., Sivanandam S., Zabludoff A. I., Zaritsky D., 2013, ApJ, 778, 14
Gunn J. E., Gott J. R., III, 1972, ApJ, 176, 1
Hester J. A., 2006, ApJ, 647, 910
Hlavacek-Larrondo J., Fabian A. C., Edge A. C., Ebeling H., Sanders J. S., Hogan M. T., Taylor G. B., 2012, MNRAS, 421, 1360
Hlavacek-Larrondo J. et al., 2014, preprint (arXiv:1410.0025)
Hughes T. M., Cortese L., 2009, MNRAS, 396, L41
Just D. W., Zaritsky D., Sand D. J., Desai V., Rudnick G., 2010, ApJ, 711, 192
Kapferer W. et al., 2007, A&A, 466, 813
Komatsu E., Seljak U., 2002, MNRAS, 336, 1256
Koopmann R. A., Haynes M. P., Catinella B., 2006, AJ, 131, 716
Lacey C., Cole S., 1993, MNRAS, 262, 627
Limousin M., Sommer-Larsen J., Natarajan P., Milvang-Jensen B., 2009, ApJ, 696, 1771
Lin Y.-T., Mohr J. J., Stanford S. A., 2003, ApJ, 591, 749
Lueker M. et al., 2010, ApJ, 719, 1045
McCarthy I. G., Bower R. G., Balogh M. L., 2007, MNRAS, 377, 1457
McDonald M. et al., 2014, ApJ, 794, 67
McNamara B. R., Nulsen P. E. J., 2007, ARA&A, 45, 117
Mantz A., Allen S. W., Rapetti D., Ebeling H., 2010a, MNRAS, 406, 1759
Mantz A., Allen S. W., Ebeling H., Rapetti D., Drlica-Wagner A., 2010b, MNRAS, 406, 1773
Merritt D., 1983, ApJ, 264, 24
Mohr J. J., Mathiesen B., Evrard A. E., 1999, ApJ, 517, 627
Moore B., Lake G., Quinn T., Stadel J., 1999, MNRAS, 304, 465
Ostriker J. P., Bode P., Babul A., 2005, ApJ, 634, 964
Parkinson H., Cole S., Helly J., 2008, MNRAS, 383, 557
Peng Y.-j., Maiolino R., 2014, MNRAS, 438, 262
Pettini M., Shapley A. E., Steidel C. C., Cuby J.-G., Dickinson M., Moorwood A. F. M., Adelberger K. L., Giavalisco M., 2001, ApJ, 554, 981
Planck Collaboration XVI, 2014, A&A, 571, A16
Planck Collaboration XX, 2014, A&A, 571, A20
Planelles S., Borgani S., Dolag K., Ettori S., Fabjan D., Murante G., Tornatore L., 2013, MNRAS
Pratt G. W. et al., 2010, A&A, 511, A85
Quilis V., Moore B., Bower R., 2000, Science, 288, 1617
Raichoor A., Andreon S., 2012, A&A, 543, A19
Rasmussen J., Ponman T. J., 2009, MNRAS, 399, 239
Sadeh S., Rephaeli Y., 2008, MNRAS, 388, 1759
Sasaki T., Matsushita K., Sato K., 2014, ApJ, 781, 36
Scannapieco E., Oh S. P., 2004, ApJ, 608, 62
Sheth R. K., Tormen G., 1999, MNRAS, 308, 119
Shimon M., Rephaeli Y., Itzhaki N., Dvorkin I., Keating B. G., 2012, MNRAS, 427, 828
Solanes J. M., Manrique A., García-Gómez C., González-Casado G., Giovanelli R., Haynes M. P., 2001, ApJ, 548, 97
Stanek R., Rasia E., Evrard A. E., Pearce F., Gazzola L., 2010, ApJ, 715, 1508
Sun M., Donahue M., Voit G. M., 2007, ApJ, 671, 190
Sun M., Voit G. M., Donahue M., Jones C., Forman W., Vikhlinin A., 2009, ApJ, 693, 1142
Tecce T. E., Cora S. A., Tissera P. B., Abadi M. G., Lagos C. D. P., 2010, MNRAS, 408, 2008
Vikhlinin A., Markevitch M., Murray S. S., Jones C., Forman W., Van Speybroeck L., 2005, ApJ, 628, 655
Vikhlinin A., Kravtsov A., Forman W., Jones C., Markevitch M., Murray S. S., Van Speybroeck L., 2006, ApJ, 640, 691
Vikhlinin A. et al., 2009, ApJ, 692, 1060
Voit G. M., Balogh M. L., Bower R. G., Lacey C. G., Bryan G. L., 2003, ApJ, 593, 272

Vollmer B., Cayatte V., Balkowski C., Duschl W. J., 2001, ApJ, 561, 708

Wechsler R. H., Bullock J. S., Primack J. R., Kravtsov A. V., Dekel A., 2002, ApJ, 568, 52

Werner N., Urban O., Simionescu A., Allen S. W., 2013, Nature, 502, 656

White S. D. M., Navarro J. F., Evrard A. E., Frenk C. S., 1993, Nature, 366, 429

Yoo J., Miralda-Escudé J., Weinberg D. H., Zheng Z., Morgan C. W., 2007, ApJ, 667, 813

Young O. E., Thomas P. A., Short C. J., Pearce F., 2011, MNRAS, 413, 691

Younger J. D., Bryan G. L., 2007, ApJ, 666, 647

Zhang Y.-Y., Finoguenov A., Böhringer H., Kneib J.-P., Smith G. P., Kneissl R., Okabe N., Dahle H., 2008, A&A, 482, 451

Zhang Y.-Y., Laganá T. F., Pierini D., Puchwein E., Schneider P., Reiprich T. H., 2011, A&A, 535, A78

APPENDIX A: PREHEATING MODEL

Our simple phenomenological preheating model is based on the analytic model of Younger & Bryan (2007). As is customary in the literature, we define entropy as

$$K = \frac{P}{\rho_g^\gamma} \,, \tag{A1}$$

where P and ρ_g are the pressure and density of the gas and γ is the adiabatic index.

For each cluster we start with the polytropic model in hydrostatic equilibrium described in Section 4.2, calculate the entropy and modify it as

$$\hat{K}(r) = K(r) + K_0, \tag{A2}$$

thus adding an entropy floor. We then solve the equation of hydrostatic equilibrium:

$$\frac{d\hat{P}}{dr} = -\frac{GM_{tot}(r)}{r^2}\hat{\rho}_g(r) \,, \tag{A3}$$

where modified quantities are denoted by hats, and the density is given by equation (A1). The temperature is then given by

$$k_B T = K^{3/5} P^{2/5} \,. \tag{A4}$$

In solving equation (A3) we choose the pressure boundary condition at the virial radius $P(R)$, such that the total gas mass is conserved (no gas outflow due to increased entropy). Relaxing this assumption will slightly modify the gas mass fraction, and in this sense the model presented here is not fully self-consistent. However, this assumption is expected to be reasonably adequate if preheating was uniform and took place long before groups and clusters formed.

This paper has been typeset from a TeX/LaTeX file prepared by the author.